Cent. Eur. For. J. 70 (2024) 156–175 sciendo DOI: 10.2478/forj-2024-0013

CENTRAL EUROPEAN Forestry Journal

ORIGINAL PAPER

Identification of drought-induced forest damage in 2022 and of its key site condition drivers through satellite imagery

Tomáš Bucha[1]*, Pavel Pavlenda[2], Bohdan Konôpka[2,3], Julián Tomaštík[4], Juliána Chudá[4], Peter Surový[3]

[1]*National Forest Centre – Forest Research Institute Zvolen, CoE LignoSilva, T. G. Masaryka 2175/22, SK-96001 Zvolen, Slovak Republic*

[2]*National Forest Centre – Forest Research Institute Zvolen, T. G. Masaryka 2175/22, SK-96001 Zvolen, Slovak Republic*

[3]*Czech University of Life Sciences Prague, Faculty of Forestry and Wood Sciences, Kamýcká 129, CZ-16500 Prague 6-Suchdol, Czech Republic*

[4]*Technical University in Zvolen, Faculty of Forestry, T. G. Masaryka 24, SK-96001 Zvolen, Slovak Republic*

Abstract

An extensive discoloration (yellowing, browning), and defoliation (leaf loss) were observed in Slovak forests during the summer of 2022. These phenomena are attributed to the combination of very low atmospheric precipitation and extremely high air temperatures from June to early August. In this study, the deterioration of forest health was analysed by comparing the image classification of Sentinel-2 satellite data from the year of intense drought occurrence, 2022, with that from a referenced year without drought occurrence, 2020. The results indicated that in 2022, the proportion of heavily damaged stands with defoliation exceeding 50% doubled, reaching 19.3% (417,000 ha), and an area of 223,000 ha experienced an increase in defoliation by 30% or more. The damage exhibited an uneven spatial distribution, with the most significant impact observed in the western and southern parts of central Slovakia, as well as partially in the southern part of eastern Slovakia. Further GIS analyses revealed that forests growing on slopes with southern aspects suffered more severe damage than with northern exposures. However, the difference between the most damaged forests with south-southeast exposure (12.2%) and the least damaged ones with north-northwest exposure (8.2%) was only 4%. The level of damage gradually decreased with increasing altitude. Nevertheless, compared to previous studies, the damage was significantly manifested even in the fourth forest vegetation zone, up to an elevation of approximately 800 m. Regarding soil texture, which influences the water regime, the damage gradually decreased with decreasing sand content, ranging from sandy soils (17.5%) to clayey soils (6.6%).

Key words: Sentinel-2 images; rainfall deficit; defoliation; climate change; abiotic environment

Editor: Roman Sitko

1. Introduction

The phenomenon of drought is increasingly and more intensely manifesting that is predominantly interpreted as an inherent aspect of climate change (e.g., Sánchez et al. 2008; Dai 2012). Drought is typically the result of a lack of precipitation and high temperatures, especially when these phenomena occur simultaneously during the vegetation period (Del-Toro-Guerrero & Kretzschmar 2020). The most easily observable signs of deteriorating tree health due to stress of various origins, including drought, are the loss or color changes of assimilation organs (Česljar et al. 2022). Due to a shortage of soil moisture, physiological stress in tree organism increases, potentially leading to irreversible tree mortality in all major forest biome ecosystems (Hammond et al. 2022). Such manifestations of climate change are becoming common also in temperate forests of Central Europe (Hlásny et al. 2014).

During the summer of 2022, extensive deterioration of the health of deciduous forests was observed in Slovakia (SHMÚ 2022). The main symptoms were changes in color (especially various types of browning) and defoliation, which were accompanied by abundant fruiting in beech and hornbeam stands. Although Eichhorn et al. (2016) and Eickenscheidt et al. (2019) indicated that higher fructification may lead to increased defoliation, the deterioration in 2022 was primarily attributed to

*Corresponding author. Tomáš Bucha, e-mail: tomas.bucha@nlcsk.org

meteorological and soil drought. The whole territory of Slovakia experienced rather extreme meteorological conditions in 2022. A large deficit of precipitation was recorded in March, and extremely dry conditions were in South-West Slovakia. The situation improved in April, and normal to moderately dry conditions prevailed until mid-May. Above-average temperatures and very limited precipitation occurred from the second half of May. In the third decade of July, an extreme drought was observed at approximately a half of meteorological stations. After precipitation events in August, it was still extremely dry in the east at the beginning of September. Soil drought mirrored meteorological conditions but was more severe in some areas. Critical soil drought began at the end of June, affecting up to 55% of the territory. By the second half of July, nearly 60% of the territory faced the extreme drought, reaching its peak on July 24th, and impacting particularly western and central Slovakia (SHMÚ 2022). Various indicators, including the climate water balance and the soil water content, confirmed the severity of the drought, especially in July. The analysis of water deficit, based on the comparison of the 2022 precipitation with the previous decadal average, revealed that in all intensive monitoring plots in Slovakia, the precipitation from May to July was less than 50% of the decadal average, with 3 out of 7 plots experiencing less than 25% of the average values (Pavlenda et al. 2022). The "InterSucho" maps in our Supplementary material (Fig. S1) document the intensity and the extent of the droughts in 2022 as well as in 2020. We used the year 2020 as a reference to compare the situation in 2022 (SHMÚ 2021a).

Considering the current millennium, the drought experienced in 2022 was not the sole episode with adverse effects on Central European forests. Notably, the most severe droughts with significant repercussions for Central European forests were documented in the years 2003 (Rebetez et al. 2006; Buras et al. 2020), 2018 (Buras et al. 2020; Rukh et al. 2023), and 2019 (Rukh et al. 2023). The main consequences of the negative impact of drought on forests include especially crown diebacks, early fruit abortions (Nussbaumer et al. 2020), early leaf senescence (Rohner et al. 2021), increased tree mortality rates in stands (Senf et al. 2020), reduced growth (Scharnweber et al. 2020), and overall production (Colangelo et al. 2018) and carbon stock loss (Somogyi 2016).

Although drought affects fine roots of trees first (causing their enhanced mortality and inhibited growth; e.g., Konôpka & Lukac 2013) and is reflected in the crown condition later, monitoring of tree's rhizosphere is challenging, and therefore it is much more suitable to focus on monitoring the condition of tree crowns. Ground-based assessment is time demanding and based on the sample survey. In contrast, satellite Earth remote sensing (ERS) can provide extensive and up-to-date data with high resolution suitable for assessing the health status of forests (Torres et al. 2021). The integration of ERS data and available GIS layers of natural and soil conditions with forest monitoring is, therefore, a current research topic for a better understanding of forest decline processes and changes in their structure due to drought.

The radiation reflected from leaves affected by water deficiency (Hunt et al. 1987; Ceccato et al. 2001), by the changes in amount of leaf biomass (Vogelmann & Rock 1988; Joria et al. 1991; Franklin et al. 2003), pigments content (Kmeť & Blaho 1996; Albrechtová et al. 2001; Zarco-Tejada et al. 2001; Wulder et al. 2008; Song et al. 2015) or surface temperature (Farella et al. 2022) can be utilized for remotely sensed forest damage assessment. These relationships between forest damage and reflected radiance have been applied to various sensors and frequency bands, primarily in the optical domain of ERS, and they are continually actualised, e.g., in the database of remote sensing indices (Henrich et al. 2009). Newly introduced Vegetation Indices (VI), in combination with proper sampling procedures and advanced algorithms, allow the identification of forest damage in the whole range from healthy to dead stands and are practically used for country-wise forest condition monitoring. Improved forest damage classification involved procedures using temporal spectral trajectories and analysing Landsat time series (Joyce & Olsson 1999; Wulder et al. 2006). Alternatively, approaches based on the difference in VI between a damaged year and a reference year were employed, achieving nearly 90% accuracy (Townsend et al. 2012). Similarly, changes in the Leaf Area Index, rather than the absolute amount of leaf biomass, were used for the country-wise bark beetle monitoring in the Czech Republic (Lukeš 2021), and changes in the Disturbance index for the assessment of the canopy cover loss after the 2018–2020 drought in Germany (Thonfeld et al. 2022), both from the Sentinel-2 time series. A two-phase sampling, integrating damage estimation and its refinement, was employed for the country-wide monitoring of forest conditions in Slovakia (Barka & Bucha 2021). In the first phase, it is based on a component optimized for damage estimation derived using the Gramm-Schmidt transformation or, alternatively, using satellite-based defoliation classifications from the previous year. The refinement is carried out by incorporating current field defoliation assessments on monitoring plots.

Data from field surveys are commonly used to validate the accuracy of forest damage assessment from satellite images. At the European level, data are collected following a uniform methodology as part of the pan-European forest health monitoring (UN-ECE ICP Forests 1994). In Slovakia, monitoring is conducted annually in a network of 112 Level I monitoring plots systematically distributed in a 16×16 km grid (Pavlenda et al. 2014; Pavlenda et al. 2022). According to Bucha et al. (2014), Barka et al. (2018), and Barka & Bucha (2021), the pixel-level defoliation estimation error ranged from ±10% to ±20% for classifications based on the ground-based refinement of the satellite estimates from 2000 to 2020, with a 68% confidence level. Based on the analysis of the achieved accuracy of forest damage classification in individual years, it is assumed that Sentinel-2 satellite images will also be suitable for the quantification of drought-induced forest damage. This can be achieved by applying a change detection analysis between years with and without drought.

The first objective of this study is to identify forest stands across the entire territory of Slovakia that experienced significant deterioration in health due to drought in the year 2022. A specific step necessary to achieve the first objective is to quantify the defoliation of forests in 2022 and compare it with the reference year 2020, during which drought did not occur. The classification of defoliation in the reference year is essential to differentiate the damage caused by drought from the damage caused by other harmful factors (e.g., biotic pests). This is based on the knowledge that spectral manifestations of damage on satellite imagery are not specific, meaning it is usually not possible to distinguish individual harmful factors based solely on the spectral reflectance in a given year (Gao et al. 2020).

The need for a comprehensive classification of drought-induced forest damage arises from the requirement for the most accurate identification of vulnerable areas. Such quantification will enable to design and subsequently implement forestry and conservation measures to minimize the risks posed by the impacts of drought on forest stands, their production and quality of produced wood. Therefore, the second objective of this work is a spatial analysis of stands identified as damaged by drought and an exploration of main predisposing site condition factors that contribute to drought-induced damage.

Based on the existing knowledge, the following hypotheses were formulated:

1. The highest intensity of forest damage caused by drought will be associated with southern exposures due to their most intense and prolonged exposure to solar energy.
2. Drought-induced forest damage will be most pronounced in areas with worse water-holding soil properties, especially on soils with a high proportion of coarse fragments and a coarser texture such as sand typical with low soil moisture retention capacity and subsequent rapid soil moisture loss.
3. Forest vegetation zones (FVZ hereinafter) at lower elevations, particularly in regions of southern Slovakia, will experience higher levels of forest damage as these areas generally receive less precipitation and higher temperatures than those at higher altitudes.

2. Material and methods

2.1. Study area

The area of interest is the entire territory of Slovakia, located in Central Europe. The territory is geographically defined by the coordinates of 47°43"–49°37" North latitude and 16°50"–22°35" East longitude.

The forest ecosystems affected by the drought in 2022 represent the research object. The subject of the research is the health condition of forest stands and the factors that affect their condition. According to the Green Report (MPRV SR 2022), forest stands, on both forest and non-forest land, cover 2.24 million hectares (1,952 + 288,000 ha), i.e. the country's forest cover is 45.7%. From the point of macroclimatic conditions, they are coniferous and deciduous forests of the temperate zone. Vertically, forests occur from about 100 m to 1,800 m above sea level. The climate has a transitional character between oceanic and continental climate with more pronounced features of continental climate. However, an altitude has the greatest influence on climatic conditions (Climate Atlas of Slovakia 2015).

The territory of Slovakia belongs geomorphologically to the sub-system of the Carpathians and the Pannonian Basin. The geological and relief diversity of the territory is also reflected in the soil conditions in terms of their chemical and physical properties. The most common soils are from the Cambisols group (almost 2/3 of the forest area). Besides, Leptosols, Luvisols, Umbrisols, Podzols, Arenosols, Planosols, according to World Reference Base for Soil Resources international system for classification of soils (WRB 2015), are also significantly represented.

The classification of forest geo-biocenoses in Slovakia for forestry is based on site conditions and the relevant forest community. Forest communities are differentiated vertically (climatic dimension) according to FVZ (Table 1) and according to edaphic-trophic conditions (edaphic dimension). The study uses the edaphic classification according to the so-called edaphic-trophic series and transitional series (from oligotrophic series A to calciphilous series D) and the waterlogged azonal geo-biocenoses with a determining influence of groundwater or stagnating surface water.

Table 1. Basic characteristics of climatically conditioned vertical distribution of forests in Slovakia expressed by forest vegetation zones (FVZ). The dominant species in the FVZ are listed in FVZ name in the reversed order.

Forest vegetation zone	Elevation (m a.s.l.)	Average annual temperature (°C)	Average amount of annual precipitation (mm)
1. Oak	< 300	> 8.5	< 600
2. Beech-oak	200–500	6.0–8.5	600–700
3. Oak-beech	300–700	5.5–7.5	700–800
4. Beech	400–800	5.0–7.0	800–900
5. Fir-beech	500–1,000	4.5–6.5	900–1,050
6. Fir-beech-spruce	900–1,300	3.5–5.0	1,000–1,300
7. Spruce	1,250–1,550	2.0–4.0	1,100–1,600
8. Dwarf pine	> 1,500	< 2.5	> 1,500
9. Azonal	—	—	—

Source: Summary information on the state of forests in the Slovak Republic 2021 (MPRV SR 2022).

2.2. Satellite images, mosaicking, calibration, and topographic normalization

Sentinel-2A and Sentinel-2B satellite images were used to classify forest damage in 2020 and 2022 using L1C processing-level products. These are radiometrically and geometrically corrected images without atmospheric correction. The products are freely available and were obtained from the Copernicus Open Access Hub (ESA, n.d.). Images from the Landsat 9 satellite were used to substitute the cloudy parts (USGS, n.d.). An overview of the used satellite images is shown in Table 2.

Table 2. Overview of satellite images used for classification of forest damage in 2020 and 2022.

Satellite platform	Sensing date	Sensing area and satellite product type	Note
Sentinel-2A	9 September 2020	Western and central Slovakia: S2A_MSIL1C_20200909T095031_N0209_R079	Cloud-free image
Sentinel-2B	21 September 2020	Central and Eastern Slovakia: S2B_MSIL1C_20200921T094039_N0209_R036	Cloud-free image
Sentinel-2A	16 September 2020	Eastern Slovakia: S2A_MSIL1C_20200916T094041_N0209_R036	Cloud-free image
Sentinel-2B	5 august 2022	Western and central Slovakia: S2B_MSIL1C_20220805T094549_N0400_R079	Cloud-free image
Sentinel-2A	4 August 2022	Eastern Slovakia: S2A_MSIL1C_20220804T093051_N0400_R136	Cloud-free image
Sentinel-2B	12 August 2022	Central and Eastern Slovakia: S2B_MSIL1C_20220812T093549_N0400_R036	Cloudy image
Landsat 9	1 August 2022	Central and Eastern Slovakia: LC09_L2SP_187026_20220801_20220803_02_T1	Cloudy image

Note: When creating the 2020 mosaic, Sentinel-2 image from 14th September 2020 was used to replace small cloud spots in the images from 9th September 2020.
When creating the 2022 mosaic, Sentinel-2 images from 21st July 2022 and 27th August 2022 were used to replace cloudy pixels in the images from 1st and 12th August 2022.

Table 3 provides a description of Sentinel-2 bands utilized for generating the Slovak mosaic of images and, subsequently for the classification of forest damage. Bands 4, 8, 11, and 12 were selected due to their higher resolution, lower sensitivity to cirrus and cirrostratus clouds, and significant spectral differences between healthy and damaged stands (Barka & Bucha et al. 2021).

Table 3. Sentinel-2 bands selected for forest damage classification in 2020 and 2022.

Sentinel-2 band	Central Wavelength (nm)	Band widths (nm)	Resolution (m)
B4 – Red	664.6	31	10×10
B8 – Visible and Near Infrared	832.8	106	10×10
B11 – Short Wave Infrared	1,613.7	91	20×20
B12 – Short Wave Infrared	2,202.4	175	20×20

The nationwide mosaic was created by combining individual satellite images. Before making the mosaic, we used the relative calibration method (Olsson 1993) to remove differences in spectral reflectance between adjacent images. The method is based on selecting a reference image to which other images were calibrated using a linear regression analysis. Regression equations were derived for each band of satellite images. We set paired values from the overlapping parts of the images classified as forest. The scenes from 9 September 2020 and 5 August 2022 were selected as the reference because they were cloud-free and covered the whole western and central part of Slovakia.

The topographic effect (slopes facing away from the sun appear darker than sun-facing slopes) was eliminated by the topographical normalization of the images using a simple statistical-empirical correction method (Teillet et al. 1982). The shading model (for the azimuth and elevation angle of the reference scenes) was derived from the digital relief model DMR3.5 with a pixel resolution of 25 × 25 m freely available on the Geoportal of the Geodetic and Cartographic Institute Bratislava.

Based on the visual interpretation, we manually masked the areas affected by clouds and shadows and then replaced them with cloud-free images from the nearest period (Table 2).

2.3. Estimation of forest damage from satellite images and field assessment

Components derived from Sentinel-2 bands by Gramm-Schmidt transformation (GST) were used for forest damage classification (Jackson 1983). The biophysical significance of the components is described in Bucha et al. (2014). The first component (NSC1 – New Synthetic Component) represents the difference between coniferous and deciduous trees. The second component of NSC2 is optimized for damage estimation. We used the NSC approach to eliminate the differences between deciduous and coniferous trees. When Sentinel bands were used directly, the influence of species composition on damage classification was evident from visual interpretation. Coniferous stands had lower defoliation than deciduous stands. Both components (NSC1, NSC2) were derived by the linear combination of 4 bands of satellite images described in Table 3.

The classification of forest condition in 2020 and 2022 was based on the principle of two-phase regression sampling (Scheer 1997). The goal of the first phase was to estimate forest damage quickly and cheaply from satellite images using the NSC2 component. The second phase aimed to refine the estimation using the field-based defoliation assessment. The obtained values were then rescaled to the defoliation range from 0% (healthy stands) to 100% (dead stands).

The field assessment was carried out during August 2020 and on August 25–26, 2022 in accordance with the ICP Forests methodology (Eichhorn et al. 2016).

The parameters of the spectral reflectance models are presented in Table 4 and Fig. 1. The model for 2020 (Fig. 1a) used 82 monitoring plots from the national network of the ICP Forest program distributed in a grid 16×16 km in Slovakia. For analyses, the average plot's defoliation was calculated from dominant or codominant trees assessed on the plot. The set was extended by 7 plots with standing dead trees, i.e. 100% defoliation, located in the High Tatra Mountains.

The model for 2022 (Fig. 1b) was based on the survey of 31 plots dominated by deciduous trees. Plots were selected in the entire range of damage, from undamaged to heavily damaged stands, and were located southwest of the town of Zvolen, specifically in the forest complex in the Javorie Mountains. At each plot, defoliation, discoloration and fructification were evaluated for 15 dominant or codominant trees closest to the centre of the plot. The average plot's defoliation was calculated and used for analyses. The set was extended by three plots with standing dead trees located in the High Tatra Mountains.

Comparing the 2020 and 2022 models, it is evident that the 2020 model suffers from the lack of severely damaged monitoring plots, with the defoliation ranging from 50% to 95%. Additionally, the field-based defoliation of two plots with NSC2 values around 73 (Fig. 1a) appears to be underestimated. However, it is more likely that the NSC2 values are increased because these plots represent pure pine stands on sandy soils with low abundance of herbaceous vegetation. This increases the reflectance and, thus, the values of the NSC2 component. The Discussion chapter presents implications for model accuracy and recommendations for the monitoring program.

2.4. Identification of forest damage caused by drought in 2022

The classification of forest damage in 2022 is the starting point for assessing the impact of drought on forest stands. To identify drought damage, we employ an approach based on comparing two assessments of the forest condition, namely one from the year without (2020) and one with the occurrence of drought (2022). The year 2021 was unsuitable for the comparison because meteorological and soil droughts were observed in the summer, significantly affecting forest stands (SHMÚ 2021b). The rate of improvement or deterioration of forest health status was quantified in % defoliation based on the difference in defoliation between 2022 and 2020. We chose 30% as a threshold value for determining substantial changes.

Table 4. Spectral reflectance models for the classification of forest damage in 2020 and 2022 by two-phase regression sampling.

Year	Model	*r*	s_{yx}	Sample size
2020	1st phase: Estimation of damage: $NSC2 = 0.376 \cdot R_{2022} - 0.478 \cdot IR_{2022} + 0.531 \cdot SWIR1_{2022} + 0.590 \cdot SWIR2_{2022}$	—	—	n1: all forests pixels
	2nd phase: Refinement of classification according to defoliation on monitoring plots $DEF_{2020} = 1.95 + 1.034 \cdot NSC2$	0.81	±12.3	n2: 89 plots
2022	1st phase: Estimation of damage: $NSC2 = 0.337 \cdot R_{2022} - 0.371 \cdot IR_{2022} + 0.669 \cdot SWIR1_{2022} + 0.550 \cdot SWIR2_{2022}$	—	—	n1: all forests pixels
	2nd phase: Refinement of classification according to defoliation on monitoring plots $DEF_{2022} = -92.17 + 1.287 \cdot NSC2$	0.87	±10.7	n2: 33 plots*

Note: *r* – correlation coefficient; s_{yx} – standard error of the regression (line); * 1 plot excluded as an outlier.

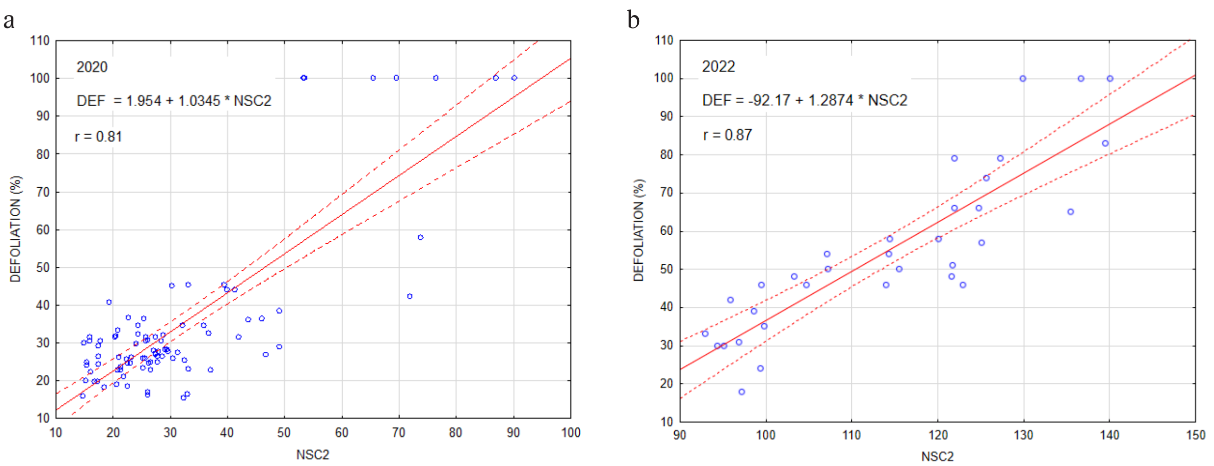

Fig. 1. Spectral reflectance models for forest damage estimation for 2020 (a) and 2022 (b). Refinement of estimation in the 2nd phase according to field assessments of defoliation at 89 plots (2020) and 33 plots (2022).
Note: Axis x: NSC2 component; Axis y: Defoliation – field evaluation of the loss of assimilation organs at plots.

A difference of ≥ 30% was considered deterioration; a difference of ≤ –30% indicated an improvement of the health status. The difference in the range from –30% to +30% was not considered as a change.

2.5. The relationship between forest damage by drought and the abiotic environment

The classifications in 2020 and 2022 and the resulting map of drought-damaged stands in 2022 were the basis for further analyses. From the forestry point of view, it is crucial to know the dependence of stand damage on site conditions in which they grow. These are given:

(i) Morphometric parameters of the relief represented in our work by exposure.
(ii) Soil environment expressed in our work by edaphic units of forest typology (so-called edaphic-trophic series) and soil texture.
(iii) Climatically conditioned vertical distribution of forest vegetation expressed in our work by FVZ.

The aspect is the direction in which the maximum slope faces. In our paper we distinguish eight aspect categories with a step of 45° starting from the north in a clockwise direction. The ninth category contains areas on plains. The whole-country exposure layer was derived in the IDRISI TerrSet from the DMR3.5 digital relief model with a pixel resolution of 25 × 25 m.

The character of the soil environment is expressed in eight categories. According to Zlatník (1976), it is a division into six edaphic-trophic series A, A/B, B, B/C, C, D and two azonal sets – a, c. These typological units reflect both chemical and physical soil conditions. Series A is oligotrophic (acid, nutrient poor soils), series B is characterised by moderately nutrient rich soils, series C is nitrophilous, with very stony soils and high humus and nitrogen content and series D is calciphilous with shallow or very stony soils. Series A/B and B/C are transitional. Two special sets (a, c) are strongly influenced by stagnant (a) or flowing (c) groundwater.

The main soil property related to its water holding capacity is the soil texture of fine earth. Soil texture classifications are based on the content of mineral fractions: clay, silt and sand. We used the classification based on the clay content (fraction under 0.01 mm) with following classes: 1 sandy, 2 loamy-sandy, 3 sandy-loamy, 4 loam, 5 clay-loamy and 6 clayey. Besides this, the content of coarse fragments (more than 2 mm) is an important parameter.

Forest vegetation zones are expressed by eight categories (Zlatník 1976). Category 9 represents all azonal communities. The basic characteristics of FVZs are shown in Table 1.

Countrywide GIS vector layers of FVZs and soil conditions were obtained from the database of the Forest Information System (NLC 2023a, b) managed by the National Forest Centre. Vector layers were rasterized and resampled together with forest damage classifications from Sentinel-2 to a pixel size of 30 × 30 m for further analyses. Hence, the area of 1 pixel was 0.09 ha.

2.6. Statistical evaluation of data

Assessing the relationships between forest damage by drought and the abiotic environment was based on the area of damaged stands and the total area of stands. The relative share of the category (w_c) was determined as the share of drought-damaged stands in the given category and the total area of the given category. The share w_c was calculated for all categories of Exposure, FVZ, Soil series and sets and Soil texture according to equation [1]:

$$w_c = \frac{A_{c\_d}}{A_{c\_all}} \qquad [1]$$

where A_{c_d} – area of the category with forest damaged by drought, A_{c_all} – total area of the category (forest without damage + forest damaged by drought).

The equation [2] was used to determine the sampling error Sp (with a 95% confidence interval) for the proportion w_c:

$$Sp = \pm 1.96 \cdot \sqrt{\frac{w\,(1-w)}{n}} \qquad [2]$$

where n – number of pixels i.e. sample size.

For the relative expression of Sp, the formula was adjusted: $Sp\,\% = Sp \cdot 100$

To determine the statistical significance of the differences in sample proportions (relative shares of the categories w_c), we established the hypothesis $H_0 : p_1 = p_2$ i.e. the proportions of the populations are equal, and the difference $w_1 - w_2$ of the sample proportions is random. To test the hypothesis, we used the test characteristic "z":

$$z = \frac{w_1 - w_2}{\sqrt{\frac{w_1\,(1-w_1)}{n_1} + \frac{w_2\,(1-w_2)}{n_2}}} \qquad [3]$$

Note: If the sample size n is large, the condition $nw\,(1-w) > 9$ applies, and the binomial distribution of the sample proportion w can be approximated by a normal distribution (Šmelko 1991; see page 154). This simplifies the confidence interval calculation for the equation [2], which is symmetric for the normal distribution.

A similar simplification also applies to hypothesis tests according to [3], when due to the size of the sample sets, the test characteristic "z" also has a normal distribution.

3. Results

3.1. Classification of forest damage

The derived reflectance models (Table 4) serve as the starting point for determining defoliation in 2020 and 2022. We applied the models to all pixels classified as forests according to the study of Bucha (1999). The analysed area was 2,160,261 ha in 2022 and 2,160,435 ha in 2020 (Table 5). A slight difference of 175 ha arose from rescaling data into the defoliation range of 0 – 100%. Pixels outside the selected thresholds were excluded from analyses as errors (e.g., remaining clouds, shadows, sensor error). The national forest condition classification results for 2020 and 2022 are presented in Fig. 2.

The accuracy of the classification can be assessed by the achieved parameters of the regression analysis (correlation coefficient, standard error of the regression line). Utilizing field assessments of defoliation in 2020 and 2022, we obtained correlation coefficients between the 1st and 2nd phases of 0.81 and 0.87, respectively. The standard error of the regression (s_{yx}) was 12.3% in 2020 and 10.7% in 2022. This implies that if the determined defoliation is 30%, it can range from 19.3% to 41.7% with 68% confidence (Table 4).

Table 5 shows the results of the 2020 and 2022 classifications, which allows the comparison of differences in defoliation classes. In addition to defoliation, a forest canopy also affects the classification of forest damage. There is a mixture of spectral properties of different categories (forest, undergrowth, herbal community, soil) in stands with an open canopy cover. For this reason, stands with different damage levels can be included in the same class of defoliation. The verbal description of the category expresses their potential difference (Table 5). The logging category in the legend represents pixels classified with defoliation > 100%.

Table 5 shows an increase in the share of heavily damaged or dead stands with defoliation above 51% in 2022 compared to 2020. This share reached 19.3%, which is approximately twofold of 2020, when it was 9.5%. In terms of area, there was an increase from 206 thousand hectares in 2020 to 417 thousand hectares in 2022. This increase indicates drought damage caused by a lack of atmospheric precipitation combined with exceptionally high air temperature values in June and July.

3.2. Spatial identification of forest damage caused by drought in 2022

The identification of stands damaged by drought was based on comparing the classifications of the forest condition in two years, one without (2020) and one with the occurrence of drought (2022). If the defoliation difference was ≥ 30%, it was considered a deterioration of the health condition in 2022 compared to 2020. Such deterioration was identified at 223,663 hectares of stands (Table 6). We remark that the terms drought-damaged stands and deterioration (by 30% and more) between 2020 and 2022 are used synonymously in the study.

Table 6. Forest condition changes between 2020–2022 due to drought in 2022. The change is expressed based on the difference in defoliation between the two years.

Category	Description of change	Change in hectares	Change in %
1	Improvement by 30% and more	33,250	1.5
2	No change or change within ±30%	1,903,390	88.1
3	Deterioration by 30% and more	223,663	10.4

Fig. 2 (bottom) depicts stands that were affected by the drought in 2022 by more than 30% in comparison to 2020. The impact was not spatially uniform, the occurrence of pixels indicating damage by drought was concentrated in the western Slovakia and the southern part of central Slovakia. Scattered individual pixels or smaller groups of pixels were also clearly visible throughout Slovakia in the image. In these cases, it mainly concerns logging realised between 2020 and 2022. According to the Green Reports on Forests (MPRV SR 2022), the logged area was approximately 30,000 ha. Changes caused by other factors, such as tending or forest fires, could also lead to

Table 5. Classification of forest damage in Slovakia according to defoliation classes – summary for 2020 and 2022.

Defoliation	2020		2022		Description of damage level in pixel
	Area (ha)	% of pixels	Area (ha)	% of pixels	
0–10%	125,419	5.8	115,103	53	No or only negligible damage
11–20%	458,524	21.2	310,457	14.4	Stands with slight damage
21–30%	718,086	33.3	621,686	28.8	
31–40%	460,645	21.3	445,290	20.6	Stands with moderate damage
41–50%	191,389	8.9	250,656	11.6	
51–60%	78,731	3.6	138,908	6.4	Stands with severe damage, disturbed areas and forest stands in regeneration
61–70%	43,890	2.0	84,089	3.9	
71–80%	27,463	1.3	60,848	2.8	
81–90%	17,837	0.8	38,901	1.8	Dying and dead stands, disturbed areas without forest regeneration, logging
91–100%	19,623	0.9	43,860	2.0	
Logging	18,829	0.9	50,463	2.4	
Total:	2,160,435	100.0	2,160,261	100.0	

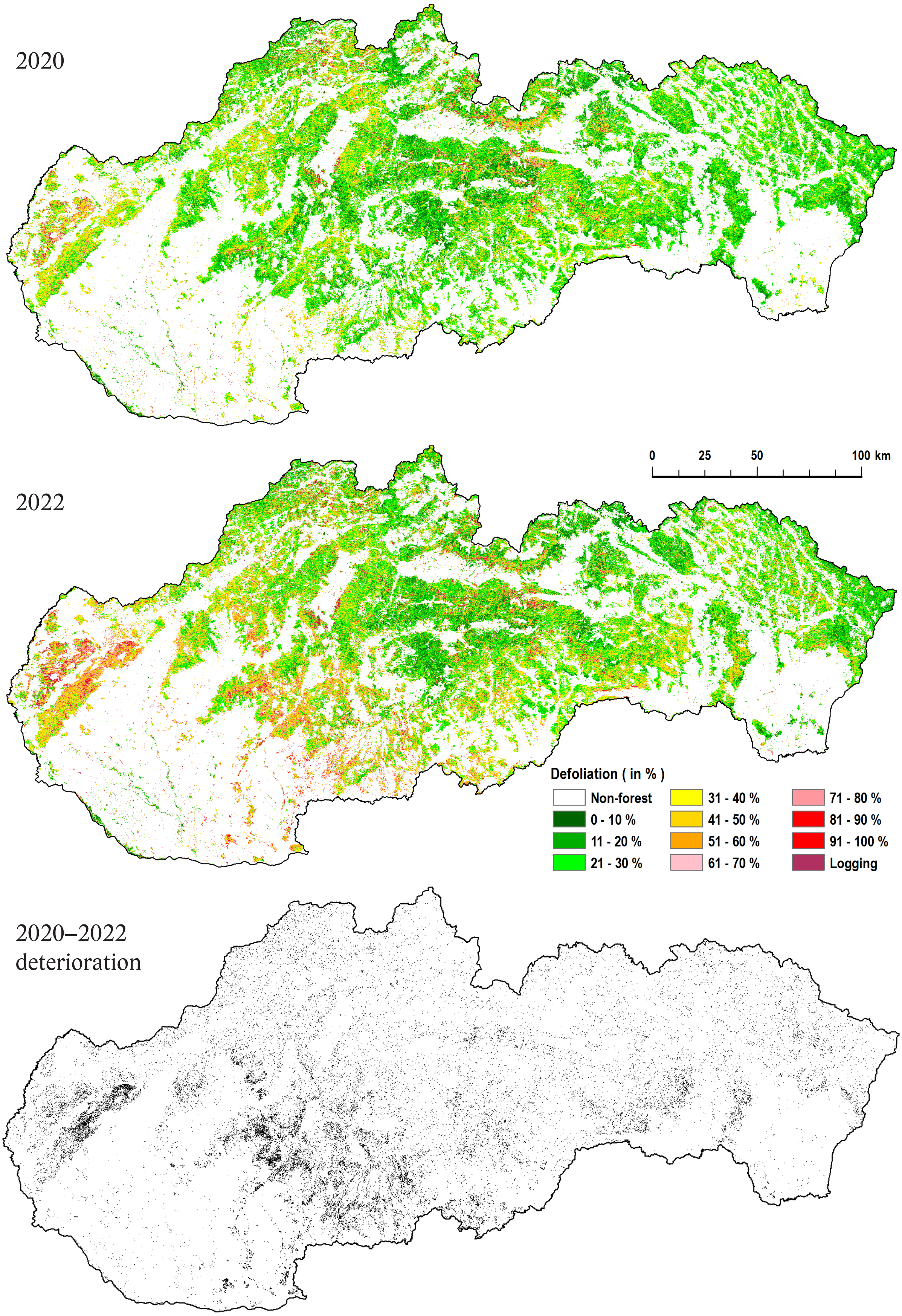

Fig. 2. Classification of forest condition in 2020 (top) and 2022 (middle) from Sentinel-2 satellite images. Bottom: Deterioration between 2020–2022 with defoliation of 30% or more.

differences greater than 30%. Affecting these areas by drought is not possible to exclude. Therefore, they were included in further analyses, in which we worked with the entire area of 223.7 thousand hectares.

3.3. The relationship between forest damage by drought and aspect

Aspect is a morphometric parameter of the relief that, through the reception of solar radiation, affects the moisture regime of soils, evapotranspiration processes and the occurrence of drought. Fig. 3 shows the relationship between the exposure of slopes divided into eight categories (at 45° steps) and the percentage of drought-damaged stands in the given category.

Table S2 (Supplementary material) shows that the areas of the analysed aspects in the Slovak Republic differ. To be able to compare the drought damage, the share of forest damage in the exposure category was calculated from the total area of forests in the given exposure category in Slovakia according to equation [1].

We recorded a gradual increase in the share (relative abundance) of forests damaged by drought from northern to southern aspects (Fig. 3). The highest proportions of damaged stands of 12.2% and 12.0% were observed on southern aspects from 135° to 180°, and from 180° to 215°. Although the occurrence of damaged stands towards northern aspects was decreasing, it was still substantial. On slopes with north-eastern aspects (from 0° to 90°) it reached 18.5%, and on northwest slopes (from 270° to 360°) 17.5%.

Regarding the area, the highest occurrences of damaged stands were observed on the SSW and WSW exposure from 180° to 270° (Table S2, Fig. 3 – line graph). However, the shift of the most damaged stands towards the western exposure is visible in the column representation in Fig. 3. This shift results from a different calculation methodology. Realistically, the highest area of damaged stands is located on the SSW and WSW exposures. However, it is also conditioned by the fact that the total area of the mentioned exposures is higher (Table S2).

To determine the vulnerability of stands according to exposures, we consider the calculation based on the ratio of the area with a damaged state of forests in a given exposure category to the total area of forests in a given exposure category more suitable. When applying this approach, the highest relative representation and, therefore, the most threatened by drought are the stands on the SSE and SSW exposures from 135° to 225° (Fig. 3 – bar graph).

3.4. The relationship between forest damage by drought and forest vegetation zones

FVZs represent changes in the composition of natural forest communities conditioned by altitudinal changes in climatic conditions. Table S1 (Supplementary material) shows the areas of drought-damaged stands in FVZs and the total area of individual FVZs in Slovakia. To mutually compare the damage to forests by drought between FVZs, the share of damage in FVZ from the total area of the given FVZ in Slovakia was calculated according to equation [1]. The resulting proportion and the area of damaged stands in FVZ are shown in Fig. 4.

The highest area representation of damaged stands was in the 3rd FVZ (69,368 hectares). This is influenced by the fact that the 3rd FVZ is the most common in Slovakia (484,485 hectares). However, the highest proportion of damaged stands (27.13%) was observed in the 1st FVZ, where the average annual temperature is the highest and the amount of precipitation is the lowest (Table S1). Fig. 4 (bar graph) shows a gradual decrease in the proportion of forest area damaged by drought with increasing FVZ.

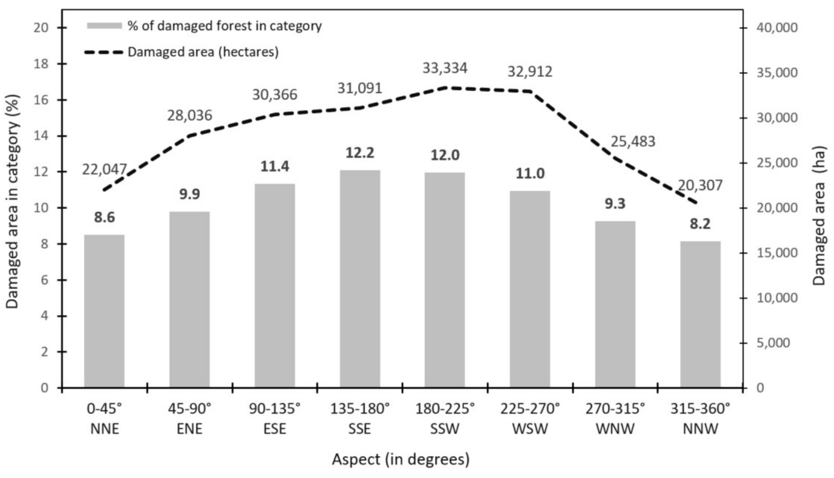

Fig. 3. Percentage of damaged stands and their area depending on the aspect. Percentage is calculated as the acreage ratio of damaged forest in the given aspect category to the total area of forests in the given aspect category.

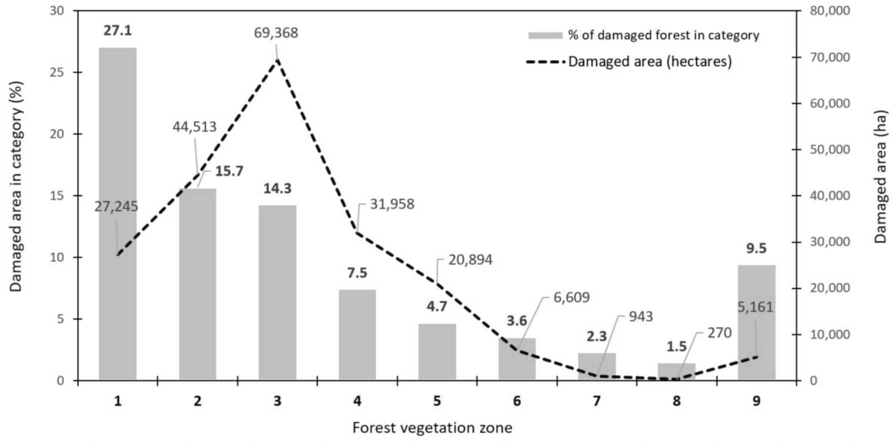

Fig. 4. Percentage of damaged stands and their area in the forest vegetation zones. FVZ: 1 – oak; 2 – beech-oak; 3 – oak-beech; 4 – Beech; 5 – fir-beech; 6 – fir-beech-spruce; 7 – Spruce; 8 – dwarf pine; 9 – azonal.

3.5. The relationship between forest damage by drought and soil properties

Edaphic-trophic series and azonal sets (ES) comprehensively represent the nature of the soil environment (soil reaction, soil humus and nutrient reserves, soil depth, contents of coarse fragments in the soil and water regime) and thus also determine the sensitivity of forest stands to drought. Table S3 (Supplementary material) shows the areas of drought-damaged stands in ES and the total area of individual ES in Slovakia. To mutually compare the damage to forests by drought between ES, the share of damage in ES from the total area of the given ES in Slovakia was calculated according to equation [1]. The shares of damaged areas and the areas of damaged stands according to ES are shown in Fig. 5.

The highest proportion of damaged forests was detected in series C, B, and D (Fig. 5). In series C and D, this is apparently related to a high proportion of coarse fragments in soils (gravels, stones, boulders), which causes their faster drying out. Series "C" is represented by strongly humic medium-deep to deep soils, which are very stony. The soils in the "D" series are shallow carbonate soils formed mainly on limestones and dolomites, usually with a high content of coarse fragments (except areas on loess). The higher proportion of damaged forest stands in series "B" may be related to its incidence at lower altitudes, which are more influenced by temperature and a lack of precipitation.

The lower occurrence of damaged stands in the transitional series A/B is related to its occurrence only at higher altitudes from the 5th FVZ, where the effect of drought is not so pronounced.

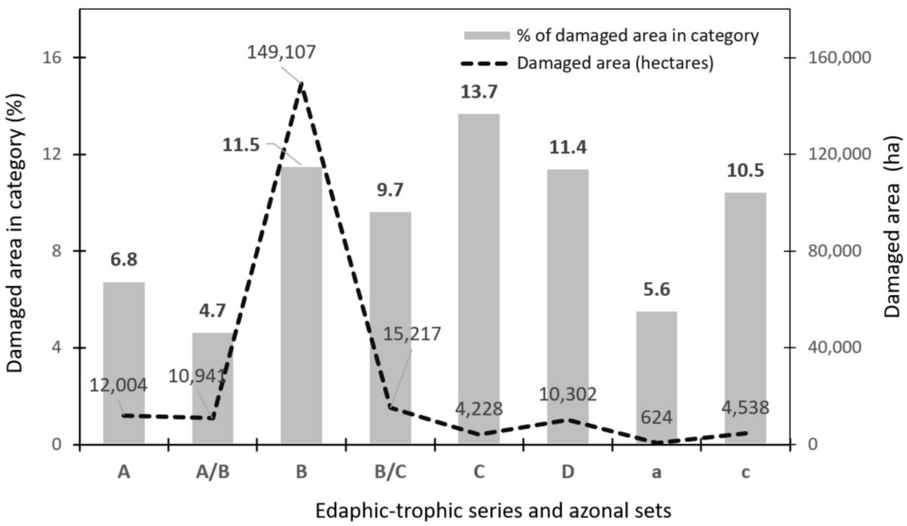

Fig. 5. Percentage of damaged stands and their area depending on the soil conditions expressed by edaphic-trophic series (A, A/B, B, B/C and D) and sets (a, c).
A – oligotrophic; B – mesotrophic; C – nitrophilous; D – calciphilous; series A/B and B/C are transitive; a – acidophilous, influenced by stagnant groundwater; c – nitrophilous, affected by flowing groundwater.

An unexpectedly high share of drought-damaged stands was also identified in set "c", which is characterized by waterlogged sites with alluvial soils at river sides. The extreme drought caused a distinct drop of water level in rivers as well as of the ground water table in soils. The gravelly substrate could cause loosening the root contact with soil water.

Even though a higher proportion of drought-damaged stands was demonstrated on soils with a greater coarse fragment content (Series C, B and D and partially also transitional B/C), the differences between the individual categories were not as distinct as we expected. To better explain the differences, we extended the analysis by another physical property of the soil, namely the influence of the granularity of the fine earth (Fig. 6; Table S4).

Fig. 6 documents a gradual decrease in the rate of forest deterioration from sandy to clayey soils, i.e. depending on the increasing proportion of the clay fraction and the decreasing proportion of the sand fraction. For Category 4, however, the proportion of deterioration was higher than for Category 3. This discrepancy is probably related to the spatial distribution of both categories in Slovakia. Sandy-loamy soils occur more frequently in a greater proportion in areas naturally less threatened by drought than loamy soils.

The analysis of the mutual interaction of the drought damage vs. edaphic-trophic series and azonal sets and soil texture showed a distinct effect of grain size on the damage even in the sets affected by groundwater, "a" and "c" (Table 7). In these sets, the upper horizons dry out in summer months in the cases of insufficient capillarity when the groundwater level drops. It is also related to water-demanding trees growing in these communities, which sensitively react to a substantial deviation in soil water saturation from the normal.

4. Discussion

4.1. Classification of forest damage and identification of drought-induced damage

The obtained forest damage classification results for 2020 and 2022 using two-stage regression sampling (Scheer 1997) confirmed the appropriateness of applying this procedure. The attained classification accuracy, expressed as the root mean square error (RMSE) of the regression line $s_{yx} = \pm 12.3\%$ (2020), resp. $s_{yx} = \pm 10.7\%$ (2022), was comparable to our previous results. Specifically, in the period from 1990 to 2021, the accuracy ranged from ±5.9% to 12.5% (Bucha et al. 2014; Barka & Bucha 2021). Our results also correspond with similar studies focusing on the estimation of defoliation.

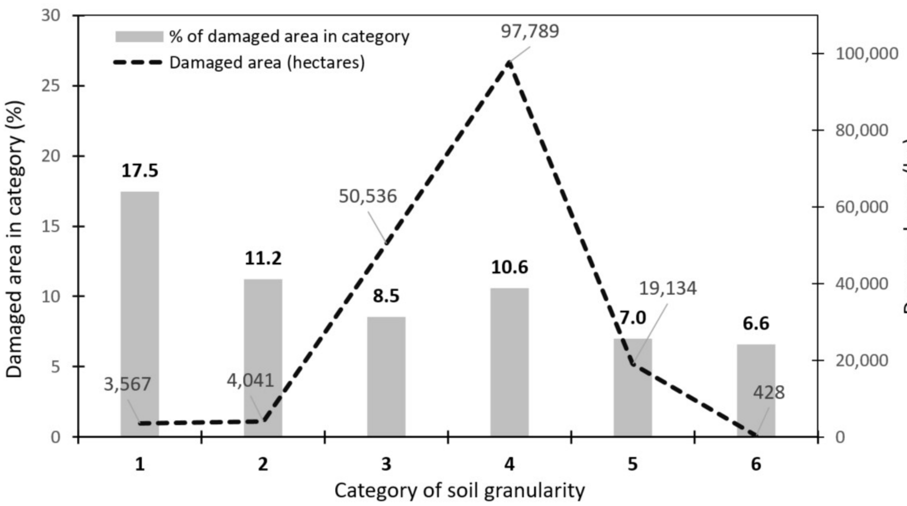

Fig. 6. Percentage of stands damaged by drought in 2022 (i.e. defoliation increased by 30% or more compared to 2020) and their area according to the granularity of forest soils.
1 – sandy soil; 2 – loamy-sandy soil; 3 – sandy-loamy soil; 4 – loamy soil; 5 – clay-loamy soil; 6 – clayey soil.

Table 7. The relative rate (%) of forest damage by drought on groundwater-affected soils in dependence to soil texture. The percentage of deterioration is calculated as the ratio of the area of damaged stands in the given category to the total forest area of the given category.

Texture of forest soils:	sandy	loamy-sandy	sandy-loamy	loam	clay-loam	clay
Code of category:	1	2	3	4	5	6
Soil set:	Percentage of stands damaged by drought (%)					
a – acidophilous, influenced by stagnant groundwater	12	9	2	2	2	3
c – nitrophilous, affected by flowing groundwater	15	14	11	9	8	3

For instance, Stoklasa & Fabiánek (1998) reported an error of ±10%, the errors presented by Ekstrand et al. (1998) ranged from ±3% to 11%, and Townsend et al. (2012) achieved an RMSE estimate of defoliation equal to ±14.9%, a mean absolute error of 10.8%, and a cross-validation R^2 of 0.805. These results demonstrate the potential of satellite monitoring for long-term monitoring of changes not only in cases of moderate to severe forest damage but also in cases of slight damage.

In addition to a comparable classification accuracy with foreign studies, the advantage of our approach is its consistency, simplicity, and cost-effectiveness based on the two-phase selection principle. These benefits arise in the first phase during the damage estimation from the unique use of GST transformation or from the national classification of forest damage from satellite images from the previous year (Barka & Bucha 2021). In the second phase, annually acquired forest monitoring data or our own ground-based assessments of defoliation are used to refine the classification. However, the 2020 model lacked monitoring plots with defoliation ranging from 50% to 95% (Fig. 1a). This caused a lower correlation coefficient and a greater standard error of estimates of the 2020 model. The average defoliation at monitoring plots in the regular network 16×16 km of the ICP Forests program ranged from 10 to 50% in "normal" years not influenced by the severe impact of damage agents. We partially overcame this problem by including the plots with standing dead stands (100% defoliation) into the model, which are easily identifiable on satellite images. Anyway, we recommend to extend annual monitoring surveys by minimally five additional plots with expected defoliation between 50–95% intentionally pre-selected based on the visual inspection of satellite images on the PC monitor to refine the estimation of damage in the first phase.

The identification of forest damage due to drought was based on the difference in defoliation between the years 2020 and 2022. According to Ognjenovic et al. (2022), a change in defoliation reflects an intense stress and represents the current or recent status of tree vitality. That is a more appropriate indicator for analysing the impact of climate conditions on forests than defoliation, which represents the accumulated impact of location-specific stressful environmental conditions on tree vitality. However, using a difference between two years involves the propagation of errors from the defoliation estimation in each year. The cumulative error is estimated at ±15%, following the principles of error propagation (Šmelko et al. 2003). The chosen threshold value of 30% for identifying worsening/improvement of the forest's health was twice the estimated error of change determination. Consequently, differences exceeding 30% can be considered significant at a 95% level.

Fig. 2 (bottom) depicts stands most significantly affected by the impacts of drought in 2022. From the map, it is evident that the influence of drought was not spatially uniform. The damage caused by drought, represented by the widespread occurrence of pixels, was concentrated in the western part of Slovakia and the southern part of central Slovakia. Stands in eastern Slovakia were less affected, although drought manifestations were observed in the southern part of the Volovské, Slanské, and Vihorlat Mountains, as well as in the Slovak Karst. We did not detect a clustered occurrence of pixels with damaged stands in the mountainous regions of northern Slovakia. These results are consistent with the spatial distribution of drought-damaged stands identified on the basis of ground monitoring of forests in a 16×16 km network in 2022 (Pavlenda et al. 2022).

The use of satellite data for monitoring forest damage in the mountainous regions of Central Europe during summer seasons is limited due to increased cloud cover and associated shadows. Affected areas need to be excluded and replaced with other available images. The shortage of optical data can be mitigated by radar with synthetic aperture radar (Bucha et al. 2021; Schellenberg et al. 2023). Therefore, a challenge for further research is to quantify the sensitivity of various microwave instruments to crown damage caused by different harmful factors, including drought.

4.2. The relationship between exposure and forest damage caused by drought

Our results confirmed the assumption of a higher occurrence of damaged stands on southern to western exposures and a decrease in the proportion of damaged stands towards northern exposures (Table S2). This observation is not novel and has been mentioned in older literature. Pfeffer et al. (1961) state that damage to stands due to drought is most common on southern and south-western exposures (180–270°). Konôpka et al. (1980) specify that the effects of drought are most pronounced on plains, on southern and south-western slopes, on limestone, sandy, and clayey soils at altitudes up to 400 to 500 meters. Similarly, Stolina et al. (1985) and Kodrík & Hlaváč (2013) noted that forest stands suffer from drought especially on southern and south-western exposures, particularly on steep slopes with shallow soils.

Our results expand upon these findings by quantifying the extent of forest damage due to drought on individual exposures (Table S2). Such quantification would be challenging to achieve through field assessments due to the difficulty of obtaining a sufficiently representative sampling set. This limitation was overcome by combining the nationwide damage assessment from satellite images with the GIS layer of exposures. The drought damage of forest stands was quantified on the entire territory of Slovakia, covering an area of 2,160,435 hectares (i.e. 24,004,833 pixels).

The large extent of the dataset, even after the categorization, influenced the statistical analysis of the data. The sampling error of determining the proportion of stands damaged by drought (*Sp*) according to equation [2] was small and ranged from 0.03 to 0.04 (Tables S2). This had an influence on the significance tests of differences in the proportion of stands damaged by drought on individual exposures according to equation [3]. All differences were statistically significant at a significance level $\alpha = 0.01$. In simpler terms, if the difference in the relative share of damaged forest on two exposures is greater than 0.1, it will be statistically significant. This finding holds not only for exposure categories but also for other analysed characteristics, such as FVZ, edaphic-trophic series and sets and soil texture (Tables S1, S3 and S4).

Although previous results reporting a higher proportion of damaged stands on S and SW exposures from 180° to 270° (28.7%) were confirmed, we found a significant level of damage on other exposures as well. On NE exposures from 0° to 90°, the proportion of stands damaged by drought was 21.3%. On NW slopes, exposures from 270° to 360°, we found a proportion of stands damaged by drought of 20.9%. The differences between the exposures were thus smaller than expected, indicating the vulnerability of forests to drought damage even on exposures less exposed to the sun.

Here, we would like to draw an attention to the difference between the results when considering exposures with 1) the highest occurrence of stands damaged by drought and 2) the most drought-endangered exposures. In the first case, the calculation is based on the area of damaged stands with a given exposure relative to the total area of damaged stands. The highest occurrence of stands damaged by drought was found on SSW and WSW exposures. This is partly due to the fact that the total area of these exposure categories is higher than that of others (Table S2). In the second case, the calculation is based on the area of damaged stands with a given exposure relative to the total area of stands with that exposure. The highest risk to stands due to drought was found on SSE and SSW exposures.

To enhance our comprehension of drought onset, further research should prioritize investigating interactions between the exposure and other geomorphic properties. The significance of slope orientation generally increases with the steepness of the geomorphic relief (Kodrik & Hlaváč 2013). The influence of geometric forms of the relief on the concentration or dispersion of the flow of substances and energy is well-known (Minár & Machová 2010), but it has not been the subject of research in terms of the effect of drought on forests, yet.

4.3. The relationship between forest vegetation zones and drought damage

Following the assumption, the highest proportion of damaged stands (27.13%) was observed in the 1st FVZ, where the average annual temperature is the highest, and the total precipitation is the lowest (Table 1). The proportion gradually decreased with increasing FVZ (Table S1). The proportion of stands damaged by drought below 5% was observed from the 5th to the 8th FVZ. The lower proportion is associated with higher annual precipitation and lower average annual temperature, attributed to an approximate decrease of –0.65 °C per 100 meters in air temperature in the troposphere with increasing elevation (Blüthgen 1980). An exception is the 9th FVZ (azonal), as forest communities in this zone are shaped by factors other than climate and occur within the entire elevational range. These communities include riparian forests, scree forests, relict pine forests, and peat bogs.

Compared to earlier studies, our results suggest a shift in drought damage up to the 4th FVZ (Fig. 4), corresponding to elevations up to 800 m above sea level, where beech forests dominantly occur. (Table 1). Pfeffer et al. (1961) found that drought damage occurred in Slovakia only up to 500 meters above sea level and related it to a decrease in average annual precipitation and an increase in average temperatures. Similarly, Konôpka et al. (1980) also mentioned that forests at elevations up to 500 meters above sea level are sensitive to drought damage. The newly discovered and quantified knowledge about the upward shift of drought-induced damage to the 4th FVZ is significant because this zone is one of the three most frequent zones in Slovakia, accounting for 21% of the total area. This highlights the vulnerability of beech forests to drought damage even at moderate elevations and is one of the first confirmations of the impact of climate change scenarios in Central Europe, as described in the study by Hlásny et al. (2014). According to the study, a significant increase in drought intensity is expected by the end of the 21st century. Large areas of southern and eastern Slovakia are projected to face an increase of 4–10 units of the Ellenberg Climatic Quotient, which had values ranging from 5 to 30 during the 1961–1990 period. The projected future conditions could represent critical conditions for the survival of drought-sensitive species. For instance, Mátyás et al. (2010) predict an intensive dieback of beech forests if the Ellenberg quotient increases by more than 13 units compared to the long-term average. Although the observed proportion of damaged stands in the 4th FVZ was not dramatically high (7.5%), the unexpected elevation distribution of damaged stands in the 4th FVZ is noteworthy. The frequency histogram of drought damage in the 4th FVZ, calculated by elevations, showed that the distribution was normal with the arithmetic mean of 617 meters above sea level, and 5–95 percentiles equal to 400–820 meters a.s.l. (Fig. S2 – Supplementary material). The occurrence of damaged stands at higher elevations can be interpreted as a signal of their potential future vulnerability.

4.4. The relationship between soil conditions and drought damage

Soil, as a complex medium composed of mineral and organic solid components, water, and gases, possesses numerous properties that influence the growing vegetation in various ways. To analyse the relationship between soil properties and forest tree damage caused by drought, we used two approaches: the classification of forest site types based on forestry typology and the classification of soil texture. In both cases, the analyses were performed across the entire territory of Slovakia. The classification of sites into edaphic-trophic series (A, A/B, B, B/C and D) and azonal waterlogged geo-biocenoses (a, c) reflects the combination of properties significantly affecting tree growth and their production potential (soil depth, stoniness, humus content, base nutrients content, nitrogen content, water regime), and, to some extent, provides better insights into the relationship between soil and trees compared to soil classification units (Pavlenda et al. 2018).

Our results confirmed the hypothesis of more pronounced forest damage on sites with soil properties (stoniness, texture, depth, humus content) that make them more susceptible to desiccation. A higher proportion of damage was found on edaphic-trophic series (B, C and D) with a higher content of coarse fragments (Fig. 5) and also on soils with a higher proportion of sand fraction (Fig. 6). According to the quantification from the National Forest Inventory data, the average content of coarse fragments in series C and D is around 69% and 45%, respectively. In other edaphic-trophic series, the average value does not exceed 33%. Soils in the series B have a coarse fragments content of up to 50% and the average content of coarse fragments is 22.9% (Bošela 2010). The high proportion of damaged forest stands may also be related to a higher proportion of B series communities in lower forest vegetation zones, which are more influenced by temperature and a lack of precipitation.

The soil texture had an obvious influence on the damage even in sets affected by groundwater "a" and "c" (Table 7), where higher sand and gravel content is the cause of the insufficient capillarity when the groundwater level drops.

The previous study on the processes leading to drought damage in Central European forests in 2018 was conducted by German researchers (Schuldt et al. 2020). Due to the extensive mortality, they hypothesized that some beech trees had reached their limit of functioning under these extreme drought conditions. This was linked to highly negative water potentials leading to embolism (Schuldt et al. 2020), which was likely the cause of a partial or complete canopy dieback. Walthert et al. (2021) found an increased stress on shallow soils with lower water holding capacity leading to embolism, which was also confirmed by Weithmann et al. (2022). Brun et al. (2020) reported early wilting and leaf shedding during the summer of 2018 in Germany and Czechia and suggested shallow soils and steep slopes are potential risk factors for such a response. A study from the Pacific Northwest USA also identified greater soil bulk density as a factor increasing forest drought sensitivity (Cartwright et al. 2020), i.e. sensitivity to drought increases from clayey to sandy soils. Our results confirmed the aforementioned findings that a higher proportion of drought-damaged stands occurs on soils more prone to drying out. At the same time, our results quantify the influence of key site condition drivers, thereby laying the groundwork for their applicability in forestry practice.

The relationship between soil, topographic, and climatic factors and drought-induced tree damage requires a further analysis of their interactions to better understand their impact on forest health. The ongoing synthesis of knowledge is equally important for the development of strategies to protect forest ecosystems against drought and climate change (but see also ClimateADAPT 2024).

It is essential to emphasize that the severity of the impact of drought on forest vegetation in Slovakia is generally underestimated, and the information on the drought-induced damage (or mortality) of forest stands is partially missing from the existing forestry evidence. This is because drought-weakened vegetation is often attacked by biotic pests, especially insects, which are easily identifiable. Therefore, foresters can visually recognize and record them, which overestimates the significance of biotic pests and, conversely, underestimates the impact of drought (Kunca et al. 2019). This is despite the well-known fact that drought and its negative consequences on temporal forests are indeed the most significant accompanying phenomena of the ongoing climate change (Pretzsch et al. 2022).

5. Conclusions

The presented results stem from the long-term research focused on classifying forest damage from satellite images. The outcome is a consistent database covering the period from 1990 to 2022, processed following a uniform methodology. This allows the comparison of the forest condition between individual years. Comparing the year 2020 with the normal precipitation, and the year 2022, which was exceptionally warm and dry, enabled the identification of forest stands that were sensitive to the manifestations of drought and extremely high air temperatures in July and early August 2022.

Linking data on forest damage from satellite images with nationwide GIS layers from the Information System of Forest Management in Slovakia allowed the modification of existing knowledge and deriving new insights into the factors influencing forests due to drought. The study analysed the rate of forest damage according to exposure, soil and soil texture properties and climatically conditioned vertical distribution of forest vegetation. To deepen our understanding of drought-induced damage, further research should focus on the categories of factors where the impact was the most significant and on analyses of their mutual interactions.

From the forestry perspective, we consider the new findings regarding forest damage caused by drought in 2022 to be highly significant and valuable. These outputs can be instrumental in proposing changes to the composition of tree species and in planning and executing silvicultural and protective measures for the management of these forest stands. To avoid the climate change-induced mortality, it may be necessary to use more drought-tolerant species for stand regeneration instead of applying the long-time general practice of native species (Somogyi 2016). It is reasonable to assume that the areas with the most extensive forest damage in 2022 are also the most drought-sensitive regions within the territory of Slovakia. Consequently, future drought episodes are likely to have the most severe impact on these areas. Therefore, forest management should proactively take this into account and make efforts to minimize the forest vegetation stress caused by drought. However, even within the existing system of differentiated forest management, which encompasses activities related to forestry planning, regeneration, silviculture, forest protection, and potentially genetics, there are notable gaps in knowledge that should be promptly addressed. These gaps need to be filled with scientific findings, which should then be rigorously tested and subsequently integrated into forestry practices. This will help enhance forest management strategies and protect forests from the adverse effects of drought and subsequent secondary (biotic) agents.

Acknowledgements

The study was co-funded by the European Commission within the LignoSilva project [Grant Agreement #101059552] under the Horizon Europe Teaming for Excellence action. The research was co-funded by the Slovak Research and Development Agency under the contracts APVV-18-0223 "Evaluation of the key properties of forest soils in Slovakia: current state, development, spatial links and relations to the state of the forest" and APVV-22-0056 "The influence of competition and other limiting factors on carbon retention and plant diversity in regenerating forest". The ground campaign was supported by the project APVV-20-0391 "Monitoring of forest stands in three-dimensional space and time using innovative approaches of close range".

References

Albrechtová, J., Rock, B. N., Soukupová, J., Entcheva, P., Šolcová, B., Polák, T., 2001: Biochemical, histochemical, structural and reflectance markers of damage in Norway spruce from the Krušné hory Mts. used for interpretation of remote sensing data. Journal of Forest Science, 47:26–33.

Barka, I., Lukeš, P., Bucha, T., Hlásny, T., Strejček, R., Mlčoušek M. et al., 2018: Remote sensing-based forest health monitoring systems – case studies from Czechia and Slovakia. Central European Forestry Journal, 64:259–275.

Barka, I., Bucha, T., 2021: Satelitné monitorovanie zdravotného stavu lesov Slovenska. In: Tóthová, S., Gergeľ, T. (eds.): Zborník odborných prác z konferencie LignoSilva 2021, konanej vo Zvolene 28. Septembra 2021. Zvolen, NLC, p. 84–92. (In Slovak).

Blüthgen, J., 1980: Allgemeine Klimageographie. Berlin, de Gruyter, 208 p. (In German).

Bošela, M., 2010: Climatic and soil characteristics of the altitudional vegetation zones and edaphic-trophic units. Lesnícky časopis – Forestry Journal, 53:215–234.

Brun, P., Psomas, A., Ginzler, C., Thuiller, W., Zappa, M., Zimmermann, N. E., 2020: Large-scale early-wilting response of Central European forests to the 2018 extreme drought. Global Change Biology, 26:7021–7035.

Bucha, T., 1999: Classification of tree species composition in Slovakia from satellite images as a part of monitoring forest ecosystems biodiversity. Acta Instituti Forestalis Zvolen, 9:65–84.

Bucha T., Barka, I., Hlásny, T., Konôpka, M., Koreň, M., Lukasová, V. et al., 2014: Satelity v službách lesa. Bratislava, SAP, 202 p. (In Slovak).

Bucha, T., Barka, I., Konôpka, B., 2021: Možnosti využitia radarových dát Sentinel-1 pri klasifikácia poškodenia lesov. In: Tóthová, S., Gergeľ, T. (eds.): Zborník odborných prác z konferencie LignoSilva 2021, konanej vo Zvolene 28. Septembra 2021. Zvolen, NLC, p. 75–83. (In Slovak).

Buras, A., Ramming, A., Zang, Ch. S., 2020: Quantifying impacts of the 2018 drought on European ecosystems in comparison to 2003. Biogeosciences, 17:1655–1672.

Cartwright, J. M., Littlefield, C. E., Michalak, J. L., Lawler, J. J., Dobrowski, S. Z., 2020: Topographic, soil, and climate drivers of drought sensitivity in forests and shrublands of the Pacific Northwest, USA. Nature. Scientific Reports, 10:18486.

Colangelo, M., Camarero, J. J., Rippulone, F., Gazol, A., Sánchez-Salguero, R., Oliva, J. et al., 2018: Drought decreases growth and increases mortality of coexisting native and introduced tree species in a temperate floodplain forest. Forests, 9:205.

Ceccato, P., Flasse, S., Tarantola, S., Jacquemoud, S., Grégoire, J. M., 2001: Detecting vegetation leaf water content using reflectance in the optical domain. Remote Sensing of Environment, 77:22–33.

Česljar, G., Jovanovič, F., Brašanec-Bosanac, L., Dordevič, I., Mitrovič, S., Eremija, S. et al., 2022: Impact of an extremely dry period on tree defoliation and tree mortality in Serbia. Plants, 11:1286.

Dai, A., 2012: Increasing drought under global warming in observations and models. Nature Climate Change, 3:52–58.

Del-Toro-Guerrero, F. J., Kretzschmar, T., 2020: Precipitation-temperature variability and drought episodes in northwest Baja California, México. Journal of Hydrology: Regional Studies, 27:100653.

Eickenscheidt, N., Puhlmann, H., Riek, W., Schmidt-Walter, P. Augustin N., Wellbrock, N. 2019: Spatial response patterns in biotic reactions of forest trees and their associations with environmental variables in Germany. In: Wellbrock, N., Bolte, A. (eds.): Status and dynamics of forests in Germany. Ecological Studies, 237. Cham, Springer, p. 311–354.

Eichhorn, J., Roskams, P., Potočić, N., Timmermann, V., Ferretti, M., Mues, V. et al., 2016: Part IV: Visual assessment of crown condition and damaging agents. Eberswalde, Germany, Thünen Institute of Forest Ecosystems, 49 p.

Ekstrand, S., Schardt, M., Granica, K., Koch, B., Kahabka, H., Carnemolla, S. et al., 1998: SEMEFOR. Satellite based environmental monitoring of European forests. EC Community research, EUR 19435, Luxembourg, 103 p.

Farella, M. M., Fisher, J. B., Jiao, W., Key, K. B., Barnes, M. L., 2022: Thermal remote sensing for plant ecology from leaf to globe. Journal of Ecology, 110:1996–2014.

Franklin, S. E., Wulder, M. A., Skakun, R. S., Carroll, A. L., 2003: Mountain pine beetle red-attack forest damage classification using stratified Landsat TM data in British Columbia, Canada. Photogrammetric Engineering & Remote Sensing, 69:283–288.

Gao, Y., Skutsch, M., Peneque-Gálvez, J., Ghilardi, A., 2020: Remote sensing of forest degradation: a review. Environmental Research Letters, 15:103001.

Hammond, W. M., Williams, A. P., Abatzoglou, J. T., Adams, H. D., Klein, T., López, R. et al., 2022: Global field observations of tree die-off reveal hotter-drought fingerprint for Earth's forests. Nature Communications, 13:1761.

Henrich, V., Jung, A., Götze, C., Sandow, C., Thürkow, D., Gläßer, C., 2009: Development of an online indices database: Motivation, concept and implementation. 6th EARSeL Imaging Spectroscopy SIG Workshop Innovative Tool for Scientific and Commercial Environment Applications. March 16–18, 2009. Tel Aviv, Israel.

Hlásny, T., Mátyás, C., Seidl, R., Kulla, L., Merganičová, K., Trombik, J. et al. 2014: Climate change increases the drought risk in Central European forests: what are the options for adaptation? Lesnícky časopis – Forestry Journal, 60:5–18.

Hunt, E. R., Rock, B. N., Nobel, P. S., 1987: Measurement of leaf relative water content by infrared reflectance. Remote Sensing of Environment, 22: 429–435.

Jackson, R. D., 1983: Spectral indices in N-Space. Remote Sensing of Environment, 13:409–421.

Joria, E. P., Ahearn, S. A., Connor, M., 1991: A comparison of the SPOT and LANDSAT Thematic Mapper 816 satellite systems for detecting gypsy moth defoliation in Michigan. Photogrammetric 817 Engineering & Remote Sensing, 57:1605–1612.

Joyce, S., Olsson, H., 1999: Long-term forest monitoring with temporal-spectral trajectories from Landsat TM data. Conference On Remote Sensing and Forest Monitoring. Rogow, Poland, p. 68–81.

Kmeť, J., Blaho, J., 1996: Obsahy fotosyntetických pigmentov v ihliciach smrekov (*Picea abies* [L.] Karst.) z rôznej nadmorskej výšky. Acta Facultatis Forestalis Zvolen, XXXVIII, p. 29–38. (In Slovak).

Kodrík, H., Hlaváč, P., 2013: Integrovaná ochrana lesa. Zvolen, Technická univerzita vo Zvolene, 328 p. (In Slovak).

Konôpka, J. et al., 1980: Smernice na ochranu lesov v Slovenskej socialistickej republike. Príroda, Bratislava, 260 p. (In Slovak).

Konôpka, B., Lukac, M., 2013: Moderate drought alters biomass and depth distribution of fine roots in Norway spruce. Forest Pathology, 43:115–123.

Kunca, A., Zúbrik, M., Galko, J., Vakula, J., Leontovyč, R., Konôpka, B. et al., 2019: Salvage felling in the Slovak Republic's forests during the last twenty years (1998–2017). Central European Forestry Journal, 65: 3–11.

Lukeš, P., 2021: Monitoring of bark beetle forest damage. In: Södergård, C., Mildorf, T., Habyarimana, E., Berre, A. J., Fernandes, J. A., Zinke-Wehlmann, Ch. (eds.): Big Data in Bioeconomy. Cham, Springer International Publishing, p. 351–361.

Mátyás, C., Berki, I., Czúcz, B., Gálos, B., Móricz, N., Rasztovits, E., 2010: Future of beech in southeast europe from the perspective of evolutionary ecology. Acta Silvatica & Lignaria Hungarica, 6:91–110.

Nussbaumer, A., Meusburger, K., Schmitt, M., Waldner, P., Gehrig, R., Haeni, M. et al., 2020: Extreme summer heat and drought lead to early fruit abortion in european beech. Scientific Reports, 10:5334.

Ognjenovic, M., Seletkovic, I., Potočic, N., Marušic, M., Perčec Tadic, M., Jonard, M. et al., 2022: Defoliation change of European beech (*Fagus sylvatica* L.) depends on previous year drought. Plants, 11:730.

Olsson, H., 1993. Regression functions for multitemporal relative calibration of thematic mapper data over Boreal forest. Remote Sensing of Environment, 46:89–102.

Pavlenda, P., Pajtík, J., Priwitzer, T., Capuliak, J., Konôpka, M., Krupová, D. et al., 2014: Monitoring lesov Slovenska. Správa za ČMS Lesy za rok 2013. Zvolen, NLC – LVÚ Zvolen, 143 p. (In Slovak).

Pavlenda, P., Sitková, Z., Šebeň, V., Capuliak, J., 2018: Návrh limitov pre udržateľné využívanie dendromasy z hľadiska nutričného stavu lesných pôd. Zvolen, Národné lesnícke centrum, 52 p. (In Slovak).

Pavlenda, P., Pajtík, P., Sitková, Z., Priwitzer, T., Pavlendová, P., 2022: Manifestations of extreme drought on forest trees species in permanent monitoring plots of PMS Forests. APOL, 3:94–101.

Pfeffer, A. et al., 1961: Ochrana lesů. Praha, SZN, 838 p. (In Czech).

Pretzsch, H., del Rio, M., Grote, H. J., Klemmt, H. J., Ordonez, C., Oviedo, F. B., 2022: Tracing drought effects from the tree to the stand growth in temperate and Mediterranean forests: insights and consequences for forest ecology and management. European Journal of Forest Research, 14:727–751.

Rebetez, M., Mayer, H., Dupont, O., Schindler, D., Gartner, K., Kropp, J. P. et al., 2006: Heat and drought 2003 in Europe: a climate synthesis. Annals of Forest Science, 63:569–577.

Rohner, B., Kumar, S., Liechti, K., Gessler, A., Ferretti, M., 2021: Tree vitality indicators revealed a rapid response of beech forests to the 2018 drought. Ecological Indicators, 120:106903.

Rukh, S., Sanders, T. G. M., Krüger, I., Schad, T., Bolte, A., 2023: Distinct responses of European beech (*Fagus sylvatica* L.) to drought intensity and length – a review of the impacts of the 2003 and 2018–2019 drought events in Central Europe. Forests, 14:14020248.

Sánchez, J. M. et al., 2008: Drought – Causes, Effects and Predictions. New York, Nova Science Publishers, Inc., 358 p.

Scharnweber, T., Smiljanic, M., Cruz-García, R., Manthey, M., Wilmking, M., 2020: Tree growth at the end of the 21st century – the extreme years 2018/19 as template for future growth conditions. Environmental Research Letters, 15:074022.

Scheer, Ľ., 1997: Assessment of forest conditions employing two-phased satellite remote sensing. International workshop: Application of remote sensing in European forest monitoring. 14th–16th October 1996. Vienna, Austria, EC, p. 337–346.

Schellenberg, K., Jagdhuber, T., Zehner, M., Hese, S., Urban, M., Urbazaev, M. et al., 2023: Potential of Sentinel-1 SAR to assess damage in drought-affected temperate deciduous broadleaf forests. Remote Sensing, 15:1004.

Schuldt, B., Buras, A., Arend, M., Vitasse, Y., Beierkuhnlein, C., Damm, A. et al., 2020: A first assessment of the impact of the extreme 2018 summer drought on Central European forests. Basic and Applied Ecology, 45:86–103.

Senf, C., Buras, A., Zang, Ch. S., Ramming, A., Seild, R., 2020: Excess forest mortality is consistently linked to drought across Europe. Nature Communications, 11:6200.

Somogyi, Z., 2016: Projected effects of climate change on the carbon stocks of European beech (*Fagus sylvatica* L.) forests in Zala County, Hungary. Forestry Journal. 62:3–14.

Song, C., Chen, J. M., Hwang, T., Gonsamo, A., Croft, H., Zhang, Q. et al., 2015: Ecological characterization of vegetation using multisensor remote sensing in the solar reflective spectrum. In: Prasad, S. T. (ed.): Remote sensing handbook Volume II: Land resources monitoring, modeling, and mapping with remote sensing (Chapter: 20). Boca Raton, Taylor & Francis Group, p. 533–575.

Stoklasa, M., Fabiánek, P., 1998: Dálkový průzkum země a pozemní šetření zdravotního stavu lesů ČR. Lesnická práce, 77:368–370. (In Czech).

Stolina, M. et al. 1985: Ochrana lesa. Bratislava, Príroda. 480 p. (In Slovak).

Šmelko, Š., 1991: Štatistické metódy v lesníctve. Zvolen, VŠLD vo Zvolene, 276 p. (In Slovak).

Šmelko, Š., Scheer, Ľ., Petráš, R., Ďurský, J., Fabrika, M., 2003: Meranie lesa a dreva. Zvolen, Ústav pre výchovu a vzdelávanie pracovníkov LVH SR Zvolen, 239 p. (In Slovak).

Teillet, P. M., Guindon, B., Goodenough, D. G., 1982: On the slope-aspect correction of multispectral scanner data. Canadian Journal of Remote Sensing, 8:84–106.

Thonfeld, F., Gessner, U., Holzwarth, S., Kriese, J., da Ponte, E., Huth, J. et al., 2022: A first assessment of canopy cover loss in Germany's forests after the 2018–2020 drought years. Remote Sensing, 14:562.

Torres, P., Rodes-Blanco, M., Viana-Soto, A., Nieto, H., Garcia, M., 2021: The role of remote sensing for the assessment and monitoring of forest health: a systematic evidence synthesis. Forests, 12:1134.

Townsend, P. A., Singh, A., Foster, J. R., Rehberg, N. J., Kingdon, C. C., Eshleman, K. N. et al., 2012: A general Landsat model to predict canopy defoliation in broadleaf deciduous forests. Remote Sensing of Environment, 119:255–265.

Vogelmann, J. E., Rock, B. N., 1988: Assessing forest damage in high-elevation coniferous forests in Vermont and New Hampshire using Thematic Mapper data. Remote Sensing of Environment, 24:227–246.

Walthert, L., Ganthaler, A., Mayr, S., Saurer, M., Waldner, P., Walser, M. et al., 2021: From the comfort zone to crown dieback: sequence of physiological stress thresholds in mature european beech trees across progressive drought. Science of the Total Environment, 753:141792.

Weithmann, G., Link, R. M., Banzragch, B. E., Würzberg, L., Leuschner, C., Schuldt, B., 2022: Soil water availability and branch age explain variability in xylem safety of european beech in Central Europe. Oecologia, 198:629–644.

Wulder, M. A., Dymond, C. C., White, J. C., Leckie, D. G., Carroll, A. L., 2006: Surveying mountain pine beetle damage of forests: A review of remote sensing opportunities. Forest Ecology and Management, 221:27–41.

Wulder, M. A., White, J. C., Coops, N. C., Butson, C. R., 2008: Multi-temporal analysis of high spatial resolution imagery for disturbance monitoring. Remote Sensing of Environment, 112:2729.

Zarco-Tejada, P. J., Miller, J. R., Noland, T. L., Mohammed, G. H., Sampson, P., 2001: Scalling-up and model inversion methods with narrow-band optical indices for chlorophyll content estimation in closed forest canopies with hyperspectral data. IEEE Transactions on Geoscience and Remote Sensing (Special Issue on Hyperspectral Remote Sensing), 39:1491–1507.

Zlatník, A., 1976: Lesnická fytocenologie. Praha, SZN, 495 p. (In Czech).

Online sources

ClimateADAPT – Adaptation option: Water sensitive forest management. Available at https://climate-adapt.eea.europa.eu/en/metadata/adaptation-options/water-sensitive-forest-management (accessed on 6 February 2024).

ESA: Sentinel-2 Mission guide. Available at https://sentinels.copernicus.eu/web/sentinel/missions/sentinel-2 (accessed on 31 August 2022).

Klimatický atlas Slovenska. Bratislava, Slovenský hydrometeorologický ústav, 2015, 132 p. MPRV SR, 2022: Správa o lesnom hospodárstve v Slovenskej republike za rok 2021 – Zelená správa. (In Slovak). Available at https://www.mpsr.sk/zelena-sprava-2022/123---18463/ (accessed on 24 June 2023).

Minár, J., Machová, Z., 2010: Učebné texty z geomorfológie. Bratislava, Univerzita Komenského v Bratislave, Prírodovedecká fakulta. (In Slovak). Available at http://fns.uniba.sk/Geomorfoskripta/ (accessed on 5 June 2023).

NLC, 2023a: Lesné pôdne jednotky. (In Slovak). Available at https://data.gov.sk/dataset/lesne-podne-jednotky (accessed on 5 June 2023).

NLC, 2023b: Lesné typologické jednotky. (In Slovak). Available on-line: https://data.gov.sk/dataset/lesne-typologicke-jednotky (accessed on 5 June 2023).

SHMÚ, 2021a: Sucho na Slovensku v roku 2020. (In Slovak). Available at https://www.shmu.sk/en/?page=2049&id=1106 (accessed on 20 June 2023).

SHMÚ, 2021b: Zhodnotenie sucha na Slovensku za rok 2021. (In Slovak). Available at https://www.shmu.sk/sk/?page=2049&id=1189 (accessed on 20 June 2023).

SHMÚ, 2022: Zhodnotenie sucha na Slovensku za rok 2022. (In Slovak). Available at https://www.shmu.sk/sk/?page=2049&id=1299 (accessed on 20 June 2023).

USGS: EarthExplore. Available at https://earthexplorer.usgs.gov/ (accessed on 31 August 2023).

WRB, 2015: World Reference Base for Soil Resources. Available at https://www.isric.org/explore/wrb (accessed on 24 June 2023).

Supplementary material

Table S1. Areal and relative proportion of health deterioration in 2022 (increase in defoliation by 30% or more compared to 2020) according to forest vegetation zones (FVZ). The relative sampling error of the proportion of deterioration corresponds to the 95% confidence interval.

Forest vegetation zone (FVZ)	Area of FVZ	FVZ area with deterioration in 2022	The ratio of deterioration to the area of FVZ in the given category and the relative sampling error
	A	*B*	$C = B \cdot 100 / A$
	(hectare)	(hectare)	(%)
1. Oak	100,434	27,245	27.13 ±0.08
2. Beech-oak	283,484	44,513	15.70 ±0.04
3. Oak-beech	484,485	69,368	14.32 ±0.03
4. Beech	427,341	31,958	7.48 ±0.02
5. Fir-beech	441,417	20,894	4.73 ±0.02
6. Fir-beech-spruce	185,955	6,609	3.55 ±0.03
7. Spruce	40,504	943	2.33 ±0.04
8. Dwarf pine	17,973	270	1.50 ±0.05
9. Azonal	54,520	5,161	9.47 ±0.08
Total:	2,036,112*	206,961	10.16 ±0.01

Note:* The lower acreage of the analysed stands is related to the missing data from the Military Forests in the National Forest Centre GIS layer. The lower acreage is observed mainly in the 1st FVZ.

Table S2. Areal and relative proportion of health deterioration in 2022 (increase in defoliation by 30% or more compared to 2020) according to exposures. The relative sampling error of the proportion of deterioration corresponds to the 95% confidence interval.

Exposure in degree	Description of exposure	Acronym	Area	Area with deterioration in 2022	The ratio of deterioration to the area in the given category and the relative sampling error
			A	*B*	$C = B \cdot 100 / A$
			(hectare)	(hectare)	(%)
0–45°	North-North-East	NNE	257,151	22,047	8.57 ±0.03
45–90°	East-North-East	ENE	284,209	28,036	9.86 ±0.03
90–135°	East-South-East	ESE	265,933	30,366	11.42 ±0.04
135–180°	South-South-East	SSE	255,845	31,091	12.15 ±0.04
180–225°	South-South-West	SSW	276,813	33,334	12.04 ±0.03
225–270°	West-South-West	WSW	299,201	32,912	11.0 ±0.03
270–315°	West-North-West	WNW	273,348	25,483	9.32 ±0.03
315–360°	North-North-West	NNW	247,449	20,307	8.21 ±0.03
Total:			2,159,950	223,578	10.35 ±0.01

Table S3. Areal and relative proportion of health deterioration in 2022 (increase in defoliation by 30% or more compared to 2020) according to soil properties expressed by Ecological series and sets. The relative sampling error of the proportion of deterioration corresponds to the 95% confidence interval.

Edaphic-trophic series and azonal sets	Area	Area with deterioration in 2022	The ratio of deterioration to the area in the given category and the relative sampling error
	A	*B*	$C = B \cdot 100 / A$
	(hectare)	(hectare)	(%)
A – Acidophilous/Oligotrophic	176,957	12,004	6.78 ±0.04
A/B – Transition from A to B	234,106	10,941	4.67 ±0.03
B – Medium nutrient (soils)	1,292,164	149,107	11.54 ±0.02
B/C – Transition from B to C	157,391	15,217	9.67 ±0.04
C – Nitrophilous	30,813	4,228	13.72 ±0.12
D – Alcalophilous /Calciphilous	90,158	10,302	11.43 ±0.06
a – Acidophilous, affected by stagnant groundwater	11,207	624	5.57 ±0.13
c – Nitrophilous, affected by flowing groundwater	43,318	4,538	10.48 ±0.09
Total:	2,036,112	206,961	10.16 ±0.01

Table S4. Areal and relative proportion of health deterioration in 2022 (increase in defoliation by 30% or more compared to 2020) according to soil texture. The relative sampling error of the proportion of deterioration corresponds to the 95% confidence interval.

Granularity code and corresponding category of soil	Area	Area with deterioration in 2022	The ratio of deterioration to the area in the given category and the relative sampling error
	A	*B*	$C = B \cdot 100 / A$
	(hectare)	(hectare)	(%)
1 – Sandy soil	20,421	3,567	17.47 ±0.16
2 – Loamy-sandy soil	36,020	4,041	11.22 ±0.10
3 – Sandy-loamy soil	591,693	50,536	8.54 ±0.02
4 – Loam soil	924,334	97,789	10.58 ±0.02
5 – Clay-loamy soil	273,924	19,134	6.99 ±0.03
6 – Clay soil	6,484	428	6.60 ±0.18
Total:	1,852,875*	175,494	9.47 ±0.01

Note:* The lower acreage of the analysed stands is related to the missing data from the Military Forests in the National Forest Centre GIS layer.

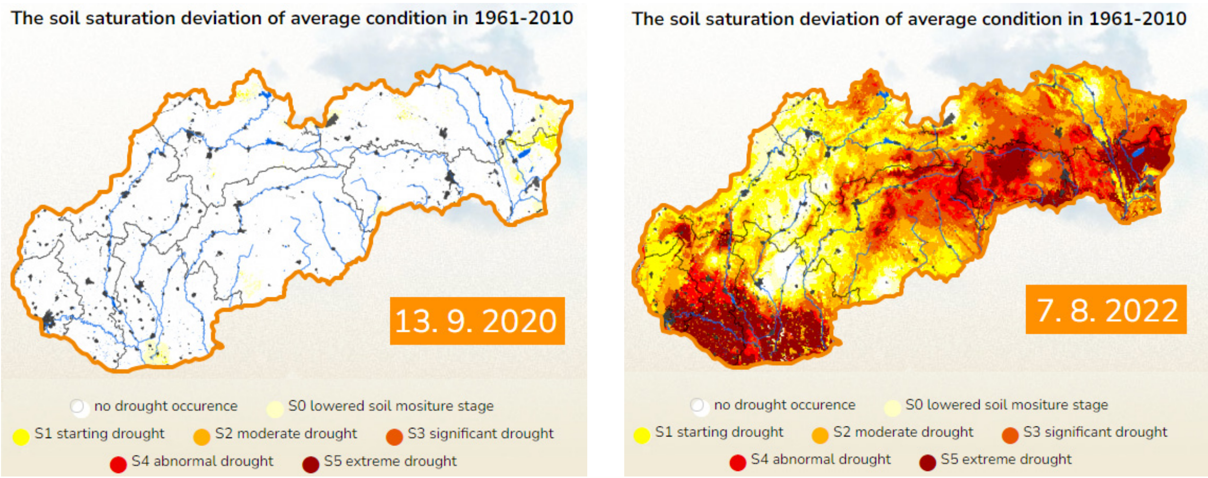

Fig. S1. The state of drought in Slovakia on 13 September 2020 and 7 August 2022. The dates correspond to the date of satellite image acquisitions used for forest damage classifications.
Source: Drought map 2020: Intersucho [online], [accessed on 2023-12-27] https://www.intersucho.sk/sk/?mapcountry=sk&from=2020-09-09&to=2020-09-16
Drought map 2022: Intersucho [online], [accessed on 2023-12-27] https://www.intersucho.sk/sk/?mapcountry=sk&from=2022-08-01&to=2022-08-10

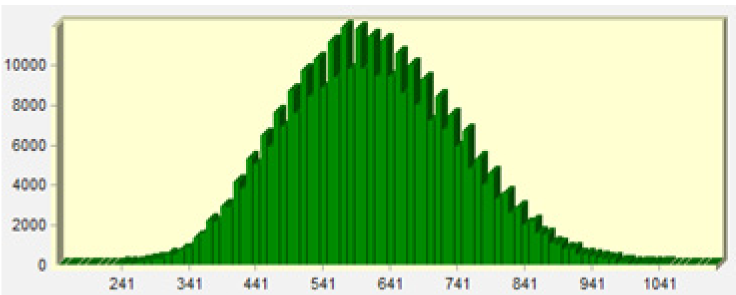

Fig. S2. The frequency histogram of drought damage in the 4th Forest vegetation zone.
Arithmetic mean of 617 meters a.s.l.; Range: 250–1,050 meters a.s.l.; 5–95th percentile: 400–820 meters a.s.l.
Note: Axis x: Altitude in meter; Axis y: Number of pixel (1 pixel – 0.09 hectares).